JACS
JOURNAL OF THE AMERICAN CHEMICAL SOCIETY

Article

pubs.acs.org/JACS

Direct Electrochemical Bioconjugation on Metal Surfaces

Ariel L. Furst,[†] Matthew J. Smith,[†] and Matthew B. Francis*[,†,‡]

[†]Department of Chemistry, University of California, Berkeley, Berkeley, California 94720-1460, United States
[‡]Materials Sciences Division, Lawrence Berkeley National Laboratories, Berkeley, California 94720-1460, United States

Supporting Information

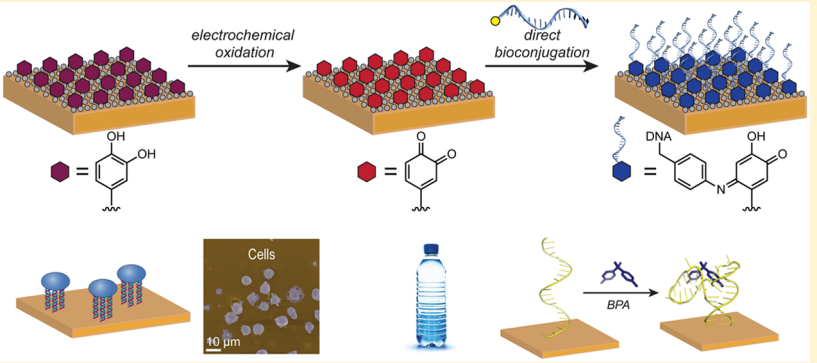

ABSTRACT: DNA has unique capabilities for molecular recognition and self-assembly, which have fostered its widespread incorporation into devices that are useful in science and medicine. Many of these platforms rely on thiol groups to tether DNA to gold surfaces, but this method is hindered by a lack of control over monolayer density and by secondary interactions between the nucleotide bases and the metal. In this work, we report an electrochemically activated bioconjugation reaction as a mild, reagent-free strategy to attach oligonucleotides to gold surfaces. Aniline-modified DNA was coupled to catechol-coated electrodes that were oxidized to *o*-quinones using an applied potential. High levels of coupling could be achieved in minutes. By changing the reaction time and the underlying catechol content, the final DNA surface coverage could be specified. The advantages of this method were demonstrated through the electrochemical detection of the endocrine disruptor bisphenol A, as well as the capture of living nonadherent cells on electrode surfaces by DNA hybridization. This method not only improves the attachment of DNA to metal surfaces but also represents a new direction for the site-specific attachment of biomolecules to device platforms.

INTRODUCTION

Nucleic acids are a privileged class of biomolecules with unmatched versatility for molecular recognition and self-assembly. Beyond their central role in living systems, synthetic oligonucleotides are essential for applications in gene detection,[1−3] specific analyte binding,[4] catalysis,[5,6] the assembly of three-dimensional structures,[7−9] and the capture of living cells bearing sequence complements.[10,11] Many of these applications depend on the coupling of DNA oligomers with inorganic surfaces, such as nanoparticles[12,13] and gold electrodes,[14] typically through thiol groups introduced at the strand termini.[15,16] Though ubiquitous, this assembly method is hindered by secondary interactions between the nucleobases and metal surfaces, which complicate the formation of well-defined, homogeneous monolayers with consistent coverage. Additionally, adequate spacing between biomolecules is critical for effective biosensing[17,18] and nanoparticle assembly applications.[19,20] Thus, a growing number of alternative synthetic approaches have involved the preassembly of mixed monolayers containing chemically active head groups,[21,22] which passivates the metal surface to prevent interactions with the DNA bases and enables control over the number of coupling sites available. Generally, a 1,3-dipolar cycloaddition of azide groups to alkynes, widely known as "Click Chemistry", provides the most common method for coupling the DNA strands to these surfaces.[17,21−24] Unfortunately, these methods can be problematic because they require redox-active catalysts that damage DNA and complicate electrochemical sensing applications or long coupling times of over 24 h. Elegant electrochemically activated couplings using *p*-quinones as Diels−Alder participants have been reported for small molecules and short peptides,[25−27] but these approaches have not been applied to the coupling of larger proteins or oligonucleotides.

Described herein is a new direct electrochemical bioconjugation reaction to couple nucleic acids to electrode surfaces with high chemoselectivity and efficiency. The reaction generates DNA monolayers in a matter of minutes without the use of additional reagents and, importantly, enables tuning of the amount of DNA coverage. The advantages of this method for preparing diagnostic platforms are highlighted through the electrochemical sensing of the endocrine disruptor bisphenol A and the capture of living, nonadherent cells on

Received: June 19, 2017

DOI: 10.1021/jacs.7b06385
J. Am. Chem. Soc. XXXX, XXX, XXX−XXX

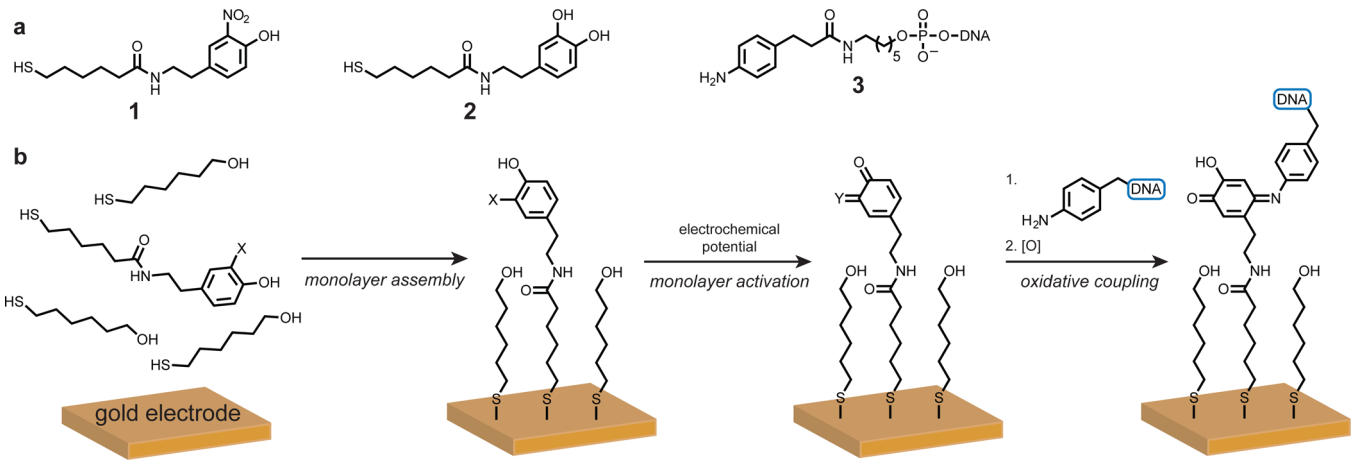

Figure 1. Overall strategy for direct electrochemical oxidative coupling on gold surfaces. (a) The structures of the coupling partners used in this study are shown. (b) Mixed monolayers containing either **1** or **2** were first formed on gold electrodes (X = NO_2 or OH; Y = O or NH). An applied potential oxidizes the coupling groups, which in turn react with anilines introduced on the DNA strands (**3**).

electrode surfaces by DNA hybridization. Both applications were found to be dependent on the surface coverage of DNA. In addition to improving the attachment of oligonucleotides to metal surfaces, this new technique represents a promising direction for the site-specific attachment of biomolecules to device platforms.

EXPERIMENTAL SECTION

General Procedure for DNA Modification of Electrodes. Catechol functionalized gold surfaces were modified with ssDNA. A 20 μL drop of 50 μM aniline-modified DNA in PBS (pH 7.2) was placed on the center of the electrode. For the rod electrodes, the gel-tip reference electrode and a platinum counter electrode were inserted into the DNA-containing liquid drop. Constant potential amperometry at a potential of 0.3 V for 240 s was generally used to attach aniline-modified DNA to the surface. For the AUTR disposable electrodes, the reference and auxiliary electrodes incorporated on the surface were used. These electrodes were activated at 0.35 V for 240 s to induce DNA coupling. Following the application of a potential, electrode surfaces were rinsed with PBS and Nanopure water. Further detail for experimental procedures is available in the Supporting Information.

Quantification of DNA on Electrode Surfaces.[17,23,40,41] DNA-modified electrodes were subjected to electrochemical measurement with 20 μM ruthenium hexammine in 0.1 M Tris buffer (pH 7.6). At this concentration of ruthenium hexammine, no signal is observed on monolayers containing no DNA and is at a concentration conventionally used for low-density DNA monolayers.[14,17,23] Cyclic voltammetry scans were obtained at a scan rate of 100 mV/s.

RESULTS AND DISCUSSION

Selection of the Coupling Partners. Previous investigations in our laboratory have explored the use of oxidative bioconjugation reactions for the rapid coupling of diverse compounds to biomolecules.[28] These strategies are dependent on the addition of anilines to *o*-iminoquinones and *o*-quinones generated *in situ* with a chemical oxidant, such as potassium ferricyanide or sodium periodate.[29−31] Protein N-termini have also been found to participate as nucleophiles in this reaction.[32] This class of reactions exhibits very high chemoselectivity and is compatible with especially low biomolecule concentrations in aqueous media. In previous work, these reactions have successfully been applied to the attachment of biomolecules to aniline-coated gold nanoparticles[33] and glass surfaces[34] in the presence of potassium ferricyanide. In addition, a photochemical version of the reaction involving azidophenols has been developed for surface patterning applications.[35]

The reliance of these reactions on the generation of an oxidized intermediate suggested that a reagent-free electrochemical variant could be developed by attaching *o*-iminoquinone or *o*-quinone precursors to electrode surfaces. To test this hypothesis, thiols **1** and **2** (Figure 1a) were prepared and combined in varying ratios with 6-mercaptohexanol. It was envisioned that the nitro group of **1** could be reduced immediately before the coupling reaction to access the *o*-iminoquinone. Monolayers were assembled on the surfaces of gold rod electrodes by exposure to ethanolic solutions of the thiol mixtures at RT for 12 h (Figure 1b). The DNA-coupling partners (**3**) were prepared through the reaction of 5′-amine terminated strands with the NHS ester of 4-azidodihydrocinnamic acid, followed by azide reduction with TCEP, as previously reported.[34]

Electrochemical Behavior of Catechol-Containing Monolayers. Surfaces coated with *o*-nitrophenols were first evaluated for the coupling reaction. Preliminary studies indicated that the nitro groups could be reduced smoothly to anilines, but the resulting *o*-aminophenol groups exhibited poor electrochemical reversibility upon subsequent redox cycling. Reductions were tested both electrochemically and using sodium dithionite. This is likely due to self-coupling of the *o*-iminoquinones with *o*-aminophenols that had not yet been reduced, a result that is consistent with the previous observation that the oxidation step is rate-limiting in these coupling reactions.[36] Previous experiments in our group have similarly observed poor reaction performance when *o*-iminoquinones are generated on polyvalent surfaces, such viral capsids. As a result, the aniline groups are typically incorporated in such locations. Although this issue could likely be solved through sufficient dilution of the *o*-nitrophenols on the gold surface, irreversible signals were observed even with 10% *o*-nitrophenol was present in the monolayer. The *o*-nitrophenol monolayers were not evaluated further.

In contrast, the electrochemical characterization of *o*-catechol-containing monolayers revealed reversible signals over multiple electrochemical cycles (Figure 2a). The consistent reversibility demonstrates that minimal self-coupling occurs between the *o*-quinones on the surface. The redox signal that does not disappear over multiple rounds of cyclic

DOI: 10.1021/jacs.7b06385
J. Am. Chem. Soc. XXXX, XXX, XXX−XXX

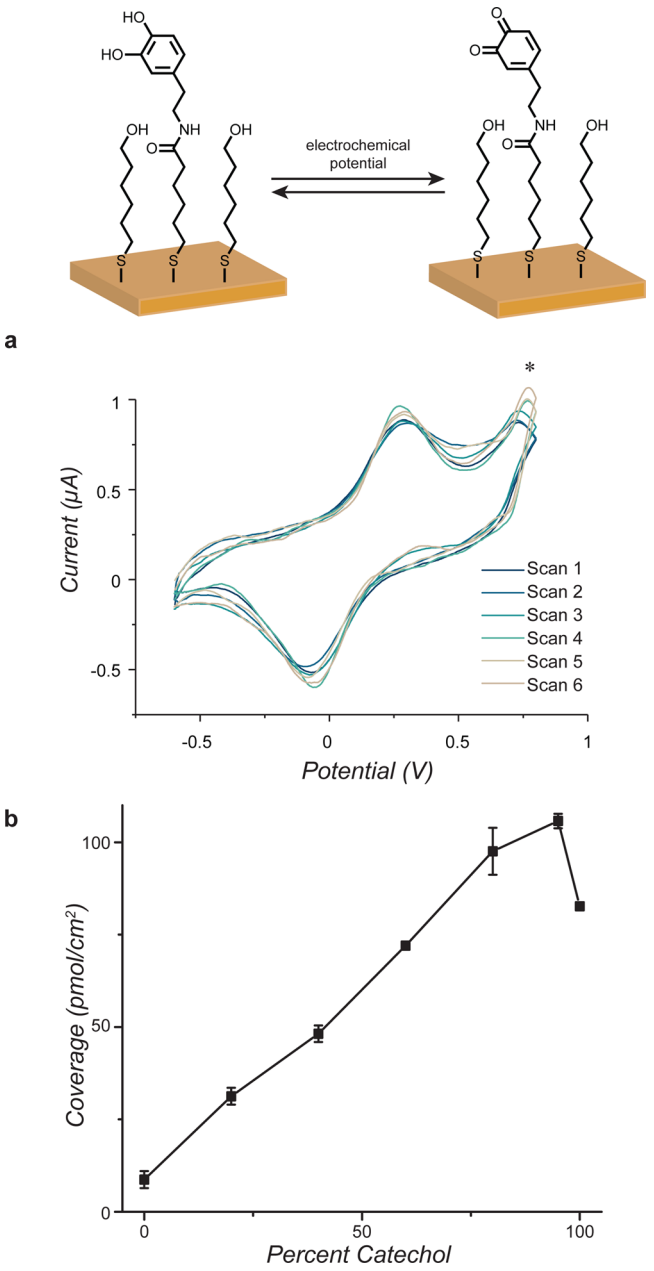

Figure 2. Electrochemical behavior of catechol monolayers. (a) Reversible oxidation occurs at a potential of 0.29 V (40% catechol). The asterisk denotes an artifact from workup and is not an independent redox peak. (b) The surface coverage of catechol can be determined using cyclic voltammetry. The number of catechol groups reflects the starting thiol ratio used for monolayer formation. Error bars represent SD for $n = 3$ replicates.

voltammetry indicates that the self-coupling occurring with the *o*-iminoquinones is likely not occurring to a large extent on these surfaces. Importantly, the final amount of catechol that assembles in a given monolayer can be controlled by varying the initial ratio of mercaptohexanol to **2**, which was quantifiable from the overall electrochemical signal from the catechol (Figure 2b and SI Figure S1). Based on literature precedent, it is hypothesized that the resultant mixed monolayer is homogeneous.[37,38] Interestingly, more catechols were incorporated using 10% 6-mercaptohexanol in the self-assembly step than when the catechol thiol was applied alone. This is likely due to improved monolayer packing by the less sterically encumbered thiol, allowing a maximum number of catechol groups to be incorporated while maintaining the lateral van der Waals interactions.[39] The maximum number of catechol groups was 105 ± 2 pmol/cm^2.

DNA Coupling to Monolayers and Quantification. Constant potential amperometry (CPA) was used to activate the catechol-modified surfaces for aniline-DNA attachment (Figure S2). The potential for activation was chosen based on the anodic peak current (310 mV versus AgCl/Ag and 350 mV versus a Ag pseudoreference). Two of the major advantages of this reaction over other chemical methods to attach DNA to preformed mixed monolayers are that this reaction is one-pot (the DNA to be coupled is added prior to oxidation of the catechol) and reagentless (no additional catalyst or oxidant is required for the reaction except for electrochemical activation). After the coupling reaction, the amount of coupled DNA was detected using ruthenium hexammine, which electrostatically interacts with the phosphate backbone of each strand.[17,40,41] Quantifying the ruthenium hexammine enabled the determination of the DNA surface coverage, which can be difficult to measure accurately using nonelectrochemical methods, such as fluorescence or radioactivity. Using this readout, the reaction was optimized for both DNA concentration and the duration of applied potential (Figure S3). Low concentrations (50 μM) of DNA yielded efficient coupling, and increasing the concentration beyond 50 μM did not improve the surface yield. The surface coverage of aniline-modified DNA was found to be proportional to the underlying catechol (Figure 3a, red trace). Maximum coupling could be achieved in 4 min, with that length of time being used for the experiments described below.

As experimental controls, no coupling was observed for unmodified DNA strands or aniline-terminated strands that had been acylated when exposed to the electrochemically activated (EC) catechol surfaces, Figure 3b. As a positive control, aniline-terminated DNA strands were also coupled to catechol surfaces without applied potential but in the presence of $K_3Fe(CN)_6$ (KFC) for 30 min, albeit it with lower overall yield. While anilines react especially rapidly with catechols, both aliphatic amines and thiols are also known to participate in the reaction at pH > 7.[31,32] The coupling efficiencies of commercially available thiol-terminated and amine-terminated DNA strands were evaluated similarly, and the DNA surface coverage was also found to be proportional to the underlying catechol coverage. In both cases, however, lower overall coverages were obtained than for aniline DNA. For thiolated duplexed DNA self-assembled as a dense monolayer, reported DNA surface coverages range from 30 to 50 pmol/cm^2. The maximum DNA coverage achieved in these experiments was 20 pmol/cm^2, which compares well with yields using strain-promoted Click coupling chemistry (but after 24 h).[17] The addition of Mg^{2+} salts to the coupling buffer was not found to influence the total amount of DNA on the surface, in contrast to surface assembly of thiolated duplexed DNA. Additionally, equal amounts of DNA were found to couple at a pH range between 7.0 and 7.5.

Formation of Whole Cell Thin Films through DNA Hybridization. The study of single cells and small groups of cells has garnered major interest in recent years because of the potential to model human diseases, such as cancer.[43] A major challenge to the study of many types of cells is their lack of innate adhesion to surfaces. Even adherent cells, which are often bound to "RGD"-coated surfaces[42] through integrin binding, require significant amounts of time or culturing to obtain confluent layers. In previous reports, we have shown that

DOI: 10.1021/jacs.7b06385
J. Am. Chem. Soc. XXXX, XXX, XXX−XXX

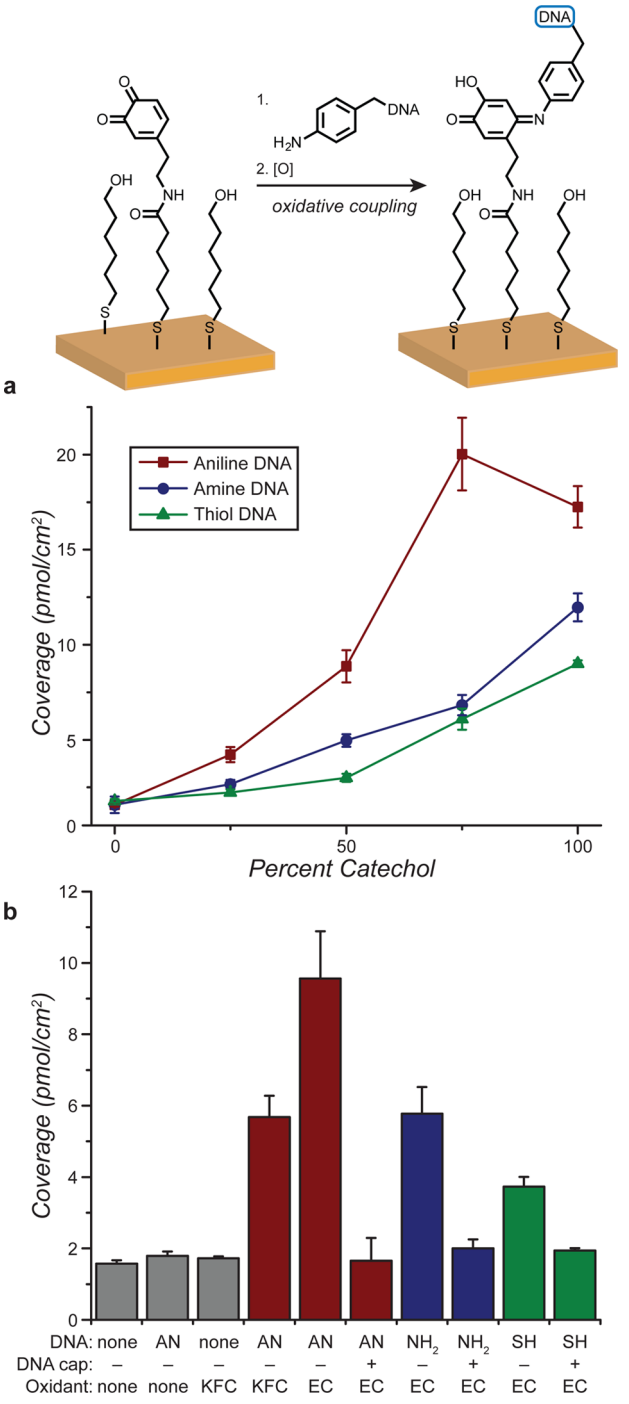

Figure 3. Electrochemical coupling of DNA strands to catechol monolayers on gold electrodes. (a) The total amount of DNA coupled to the surface was found to depend on the percentage of catechol in the monolayer. (b) DNA strands with different 5′-functional groups (none = OH, AN = aniline, NH_2 = aliphatic amine, SH = thiol) were exposed to gold surfaces coated with catechols from a 50% starting thiol mixture. Some strands were capped (*p*-iminoquinone for AN, acetyl for NH_2, and maleimide for SH) to block the terminal functional groups. To couple the strands, a potential of 0.31 V was applied for 240 s (EC), or 2 mM $K_3Fe(CN)_6$ (KFC) was added for 30 min. The surface DNA was quantified using ruthenium(III) hexammine. Error bars represent SD for $n = 3$ replicates.

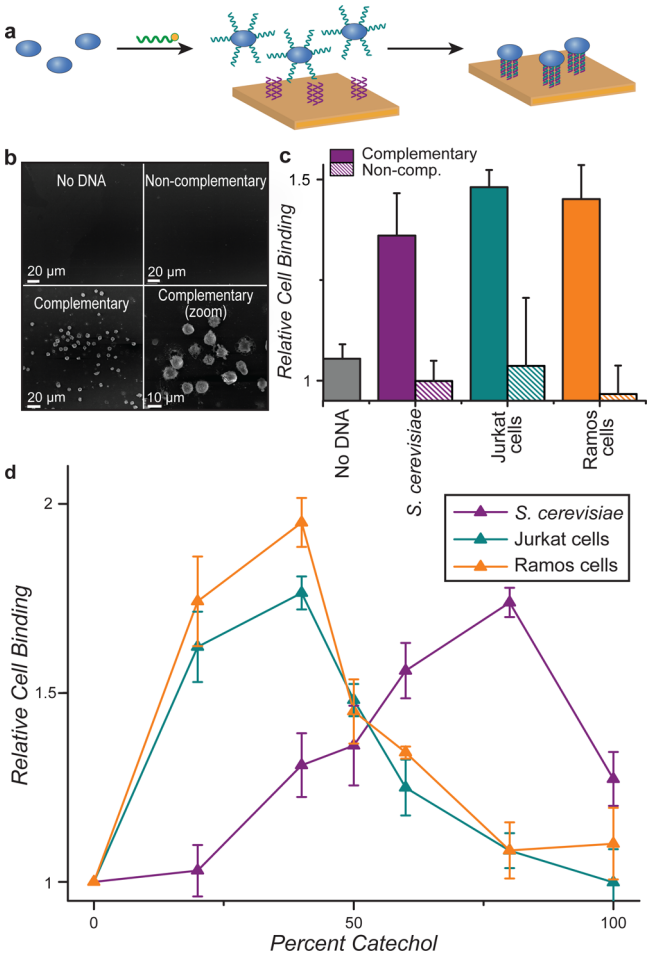

Figure 4. Attaching living cells to DNA-functionalized gold electrodes. (a) Synthetic DNA strands were attached to the surfaces of yeast and nonadherent mammalian cells. The cells attach to surfaces bearing complementary sequences. (b) SEM micrographs of Ramos cells on transparent gold electrodes. (c) Cell adhesion was dependent on the presence of the proper complement. (d) The optimal amount of surface DNA varied by cell type. Error bars represent SD for $n = 3$ replicates.

live cells can be modified to display synthetic DNA strands on their surfaces, allowing their efficient capture by surfaces bearing the strand complements, Figure 4a.[10,11,44] This technology was originally developed on gold surfaces,[10] but low levels of cell coverage were observed. The use of the electrochemical oxidative coupling method to introduce the capture strands is advantageous for this application because it allows both the control and the quantitation of the DNA strands on the surface. This allows the effects of capture strand density on cell binding efficiency to be determined for the first time.

The surfaces of three different cell types were modified with a particular sequence of DNA, and catechol-substituted, optically transparent gold electrodes were modified with varying amounts of the complementary strand as described above. Nonadherent mammalian cells (Jurkat and Ramos) were tested, as were *Saccharomyces cerevisiae*.[45] The cells were treated with fluorescein diacetate prior to imaging to allow quantitation using fluorescence imaging. To observe the cell morphology after binding, the mammalian cells were subsequently fixed on electrode surfaces and imaged by scanning electron microscopy (SEM, Figure 4b).

In each case, the cells were observed to bind to the electrode surfaces when the correct strands were present. Surfaces

DOI: 10.1021/jacs.7b06385
J. Am. Chem. Soc. XXXX, XXX, XXX−XXX

bearing no capture strands or noncomplementary sequences (identical sequences, sequence C2, on both the cells and the electrode surface) did not bind to the cells (Figure 4b,c). As has been previously reported, the cells maintained their morphology upon binding to electrodes via DNA hybridization.

Interestingly, the optimal DNA coverage for cell capture was found to vary by cell type, Figure 4c. Both Jurkat and Ramos cells were found to bind optimally to electrodes prepared with an underlying catechol concentration of ~40%. In contrast, *S. cerevisiae* were found to bind optimally to DNA surfaces with underlying catechol concentrations of ~80%. The ability of the mammalian cells to bind to surfaces with a lower DNA coverage is likely due to the greater overall number of DNA contacts that can be formed over their larger contact area, relative to yeast. This effect was seen for both Ramos and Jurkat cells. All three cell types exhibited reduced binding efficiency at the highest levels of DNA coverage, possibly due to increased levels of strand repulsion with the excess unbound strands. The larger degree of negative charge on surfaces with high DNA coverage could also serve to repel the negatively charged mammalian cell surfaces more strongly than the yeast. While these effects are under continued investigation, these experiments clearly show the benefit of being able to tune and determine the DNA density for optimal cell binding.

Specific Detection of BPA Using an Electrode-Bound Aptamer. Bisphenol A (BPA) is a component of plastics and epoxies, many of which are used for food or beverage storage. BPA is an agonist for the human estrogen receptor α (ERα) and binds to this receptor with a low-micromolar affinity, making concentrations of ppm potentially problematic. Studies have implicated this compound in a variety of disorders and diseases, including obesity, infertility, early puberty, and cancer.[46,47] Because of its ubiquity and potential for detrimental effects on human health, its rapid and facile detection is of the utmost importance. To date, most techniques for the detection of BPA either rely on the detection of total estrogenic activity[48,49] of a sample or on chromatographic-based separations.[50,51] Aptamers offer sensitivity and selectivity without some of the difficulties associated with the application of antibodies for detection.

In previous work, a DNA aptamer has been reported for the selective binding of BPA detected by electrochemical sensing on carbon nanotube–gold nanoparticle composites.[52] Conformational changes in the DNA strand occurring upon BPA binding increase surface blocking, therefore producing a detectable electrochemical signal. The reported detection limit with these composite nanorods was sub-nanomolar, yet this method of detection was not evaluated on a 2-dimensional electrode. It has previously been reported that 3-dimensional features on electrode surfaces alter both coverage and detection limits.[53] To test the compatibility of this detection system both with 2-dimensional, commercial electrodes and with the direct electrochemical coupling technique, the BPA aptamer sequence was appended with an aniline moiety and coupled to the catechol monolayers at 310 mV for 4 min. Quantification using ruthenium hexammine indicated a coverage of 18 ± 1.2 pmol/cm^2. Following electrode preparation, the electrochemical response to BPA was monitored by square wave voltammetry (SWV) with $Fe(CN)_6^{3-/4-}$ in solution, which was used to minimize the capacitance in the signal and maximize the signal-to-noise ratio. As BPA was added, the signal decreased (Figure 5a, inset). The original reference for this aptamer provides a hypothesis for its function. Briefly, the conformational change

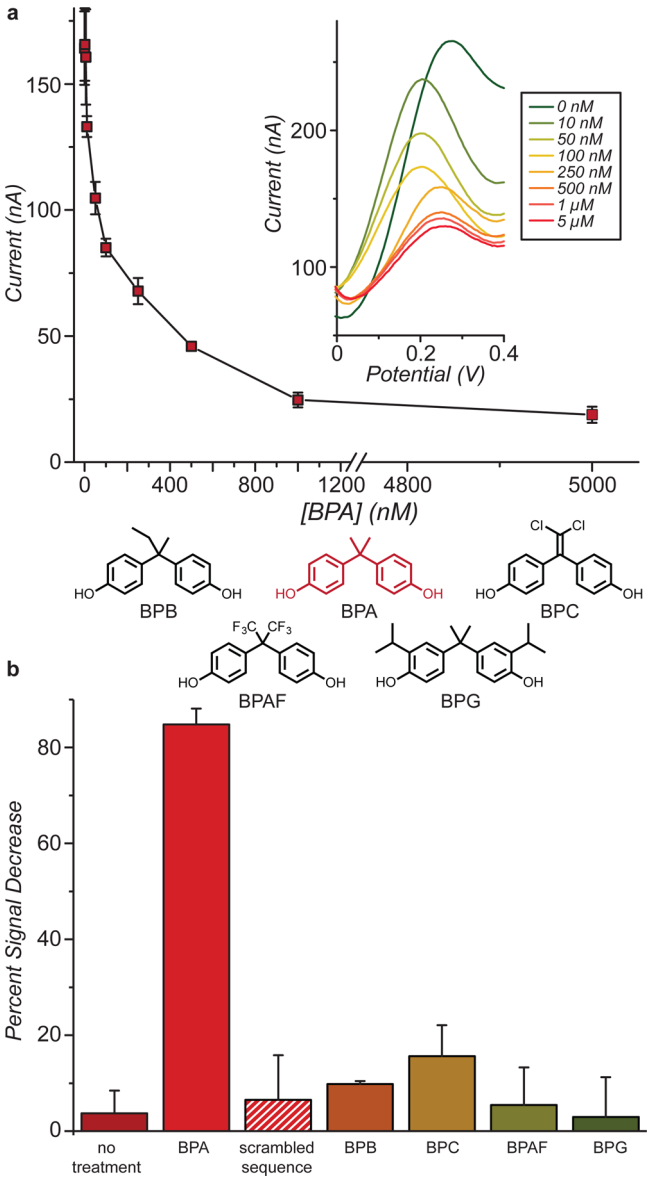

Figure 5. Specific detection of bisphenol a (BPA) using DNA aptamers oxidatively coupled to gold electrodes. (a) The current varied with the concentration of BPA. The inset shows the square wave voltammetry data, and the larger graph reports the maximum peak currents observed. (b) The response was specific for BPA and depended on the aptamer sequence. Error bars represent SD for $n = 3$ replicates.

in the aptamer sequence upon BPA binding is reported to block more of the surface from the especially high concentration of ferricyanide. As more BPA binds, more of the surface is blocked due to rigidification of the aptamer.[52] The concentration of $Fe(CN)_6^{3-/4-}$ in solution was optimized such that the surface was not passivated against it prior to BPA addition, but upon BPA addition, passivation increased, decreasing the observed signal. The maximum peak height (current) from SWV was found to depend on BPA concentration (Figure 5a). Concentrations as low as 50 nM could be detected clearly (1 pmol of BPA in a 20 μL sample). Based on the data obtained, the detection limit of our system was 10 nM, with a dynamic range of 10 nM to 5 μM, well within the biologically relevant range of BPA contamination. The linear range of the sensor is from 10 nM to 1 μM with concentration on a logarithmic scale.

DOI: 10.1021/jacs.7b06385
J. Am. Chem. Soc. XXXX, XXX, XXX–XXX

The aptamer-based BPA detection was found to be sequence-specific; a scrambled aptamer sequence was tested, and no signal decrease was observed upon BPA addition (Figure 5b). Furthermore, exposure of the electrodes to bisphenol B, C, AF, and G (BPB, BPC, BPAF, and BPG, each at 1 μM) confirmed that the binding specificity of the aptamer sequence was maintained upon surface attachment. As with cell adhesion, an optimal surface coverage of DNA was found for BPA detection; if DNA coverage was not at the optimal level, signal decrease was significantly attenuated in the presence of BPA (starting with a 75% catechol monolayer, Figure S5).

This electrochemically activated coupling method is ideal for surface modification due to its ease of use, biocompatibility, and reagentless surface activation. It also has a unique ability to establish and quantify the level of DNA coverage, which was found to be advantageous for multiple applications. The efficiencies of both cell adhesion through DNA hybridization and BPA detection by DNA aptamers were found to depend greatly on the surface coverage of DNA, with individual optimization necessary for each situation. We have optimized surfaces for the binding of three nonadherent cell types: Jurkat cells, Ramos cells, and *S. cerevisiae*. Additionally, especially low concentrations of BPA were detected with our platform using optimized DNA aptamer-modified electrodes. It is likely that this convenient method will find use for many different applications that require well-defined DNA monolayers on conductive surfaces.

Moreover, the oxidative coupling reactions themselves offer proven compatibility with a very wide range of molecules, including peptides, proteins, polymers, and nanoparticles, and can proceed rapidly at very low concentrations. This generality in other contexts suggests that the direct electrochemical coupling method could be expanded to generate functional monolayers with widely varying compositions and functions. The continued efforts toward the exploration and expansion of this new chemical technique are currently underway.

■ ASSOCIATED CONTENT

Supporting Information

The Supporting Information is available free of charge on the ACS Publications website at DOI: 10.1021/jacs.7b06385.

Methods and materials, cyclic voltammetry and electrochemical activation of catechol-modified electrodes, optimization of aniline−DNA attachment to catechol electrodes, images of cell-modified electrodes, optimization of BPA detection, and current density for detection of BPA using DNA aptamers (PDF)

■ AUTHOR INFORMATION

Corresponding Author

*mbfrancis@berkeley.edu

ORCID

Matthew B. Francis: 0000-0003-2837-2538

Notes

The authors declare no competing financial interest.

■ ACKNOWLEDGMENTS

This work was supported by Agilent and the NSF (Grant CHE-1413666). A.L.F. was supported by the A. O. Beckman Postdoctoral Fellowship. M.J.S. was supported by NSF SAGE IGERT program.

■ REFERENCES

(1) Chee, M.; Yang, R.; Hubbell, E.; Berno, A.; Huang, X. C.; Stern, D.; Winkler, J.; Lockhart, D. J.; Morris, M. S.; Fodor, S. P. *Science* **1996**, *274*, 610.

(2) Lipshutz, R. J.; Fodor, S. P. A.; Gingeras, T. R.; Lockhart, D. J. *Nat. Genet.* **1999**, *21*, 20.

(3) Lockhart, D. J.; Winzeler, E. A. *Nature* **2000**, *405*, 827.

(4) Hermann, T.; Patel, D. J. *Science* **2000**, *287*, 820−825.

(5) Breaker, R. R.; Joyce, G. F. *Chem. Biol.* **1994**, *1*, 223.

(6) Elbaz, J.; Lioubashevski, O.; Wang, F.; Remacle, F.; Levine, R. D.; Willner, I. *Nat. Nanotechnol.* **2010**, *5*, 417.

(7) Rothemund, P. W. K. *Nature* **2006**, *440*, 297.

(8) Dietz, H.; Douglas, S. M.; Shih, W. M. *Science* **2009**, *325*, 725.

(9) Aldaye, F. A.; Palmer, A. L.; Sleiman, H. F. *Science* **2008**, *321*, 1795.

(10) Chandra, R. A.; Douglas, E. S.; Mathies, R. A.; Bertozzi, C. R.; Francis, M. B. *Angew. Chem., Int. Ed.* **2006**, *45*, 896.

(11) Douglas, E. S.; Chandra, R. A.; Bertozzi, C. R.; Mathies, R. A.; Francis, M. B. *Lab Chip* **2007**, *7*, 1442.

(12) Mirkin, C. A.; Letsinger, R. L.; Mucic, R. C.; Storhoff, J. J. *Nature* **1996**, *382*, 607.

(13) Alivisatos, A. P.; Johnsson, K. P.; Peng, X.; Wilson, T. E.; Loweth, C. J.; Bruchez, M. P.; Schultz, P. G. *Nature* **1996**, *382*, 609.

(14) Drummond, T. G.; Hill, M. G.; Barton, J. K. *Nat. Biotechnol.* **2003**, *21*, 1192.

(15) Herne, T. M.; Tarlov, M. J. *J. Am. Chem. Soc.* **1997**, *119*, 8916.

(16) Kelley, S. O.; Jackson, N. M.; Hill, M. G.; Barton, J. K. *Angew. Chem., Int. Ed.* **1999**, *38*, 941.

(17) Furst, A. L.; Hill, M. G.; Barton, J. K. *Langmuir* **2013**, *29*, 16141.

(18) Soleymani, L.; Fang, Z.; Sargent, E. H.; Kelley, S. O. *Nat. Nanotechnol.* **2009**, *4*, 844.

(19) Jin, R.; Wu, G.; Li, Z.; Mirkin, C. A.; Schatz, G. C. *J. Am. Chem. Soc.* **2003**, *125*, 1643.

(20) Myers, B. D.; Lin, Q.-Y.; Wu, H.; Luijten, E.; Mirkin, C. A.; Dravid, V. P. *ACS Nano* **2016**, *10*, 5679.

(21) Collman, J. P.; Devaraj, N. K.; Chidsey, C. E. D. *Langmuir* **2004**, *20*, 1051.

(22) Devaraj, N. K.; Miller, G. P.; Ebina, W.; Kakaradov, B.; Collman, J. P.; Kool, E. T.; Chidsey, C. E. D. *J. Am. Chem. Soc.* **2005**, *127*, 8600.

(23) Pheeney, C. G.; Barton, J. K. *Langmuir* **2012**, *28*, 7063.

(24) Furst, A. L.; Hill, M. G.; Barton, J. K. *Langmuir* **2015**, *31*, 6554.

(25) Yousaf, M. N.; Mrksich, M. *J. Am. Chem. Soc.* **1999**, *121*, 4286.

(26) Yousaf, M. N.; Chan, E. W. L.; Mrksich, M. *Angew. Chem., Int. Ed.* **2000**, *39*, 1943.

(27) Mlcoch, J.; Steckhan, E. *Tetrahedron Lett.* **1987**, *28*, 1081.

(28) ElSohly, A. M.; Francis, M. B. *Acc. Chem. Res.* **2015**, *48*, 1971.

(29) Hooker, J. M.; Esser-Kahn, A. P.; Francis, M. B. *J. Am. Chem. Soc.* **2006**, *128*, 15558.

(30) Behrens, C. R.; Hooker, J. M.; Obermeyer, A. C.; Romanini, D. W.; Katz, E. M.; Francis, M. B. *J. Am. Chem. Soc.* **2011**, *133*, 16398.

(31) Obermeyer, A. C.; Jarman, J. B.; Netirojjanakul, C.; El Muslemany, K.; Francis, M. B. *Angew. Chem., Int. Ed.* **2014**, *53*, 1057.

(32) Obermeyer, A. C.; Jarman, J. B.; Francis, M. B. *J. Am. Chem. Soc.* **2014**, *136*, 9572.

(33) Capehart, S. L.; ElSohly, A. M.; Obermeyer, A. C.; Francis, M. B. *Bioconjugate Chem.* **2014**, *25*, 1888.

(34) Palla, K. S.; Hurlburt, T. J.; Buyanin, A. M.; Somorjai, G. A.; Francis, M. B. *J. Am. Chem. Soc.* **2017**, *139*, 1967.

(35) El Muslemany, K. M.; Twite, A. A.; ElSohly, A. M.; Obermeyer, A. C.; Mathies, R. A.; Francis, M. B. *J. Am. Chem. Soc.* **2014**, *136*, 12600.

(36) ElSohly, E. M.; MacDonald, J. I.; Hentzen, N. B.; Aanei, I. L.; El Muslemany, K. M.; Francis, M. B. *J. Am. Chem. Soc.* **2017**, *139*, 3767.

(37) Chidsey, E. D.; Bertozzi, C. R.; Putvinski, T. M.; Mujsce, A. M. *J. Am. Chem. Soc.* **1990**, *112*, 4301.

(38) Folkers, J. P.; Laibinis, P. E.; Whitesides, G. M. *J. Adhes. Sci. Technol.* **1992**, *6*, 1397.

(39) Ulman, A. *Chem. Rev.* **1996**, *96*, 1533.

DOI: 10.1021/jacs.7b06385
J. Am. Chem. Soc. XXXX, XXX, XXX−XXX

(40) Steel, A. B.; Herne, T. M.; Tarlov, M. J. *Anal. Chem.* **1998**, *70*, 4670.
(41) Ceres, D. M.; Udit, A. K.; Hill, H. D.; Hill, M. G.; Barton, J. K. *J. Phys. Chem. B* **2007**, *111*, 663.
(42) Ruoslahti, E.; Pierschbacher, M. D. *Science* **1987**, *238*, 491.
(43) Todhunter, M. E.; Jee, N. Y.; Hughes, A. J.; Coyle, M. C.; Cerchiari, A.; Farlow, J.; Garbe, J. C.; LaBarge, M. A.; Desai, T. A.; Gartner, Z. J. *Nat. Methods* **2015**, *12*, 975.
(44) Hsiao, S. C.; Shum, B. J.; Onoe, H.; Douglas, E. S.; Gartner, Z. J.; Mathies, R. A.; Bertozzi, C. R.; Francis, M. B. *Langmuir* **2009**, *25*, 6985.
(45) Twite, A. A.; Hsiao, S. C.; Onoe, H.; Mathies, R. A.; Francis, M. B. *Adv. Mater.* **2012**, *24*, 2380.
(46) Tsai, W.-T. *J. Environ. Sci. Health C* **2006**, *24*, 225.
(47) Rochester, J. R. *Reprod. Toxicol.* **2013**, *42*, 132.
(48) Paech, K.; Webb, P.; Kuiper, G. G. J. M.; Nilsson, S.; Gustafsson, J.-A.; Kushner, P. J.; Scanlan, T. S. *Science* **1997**, *277*, 1508.
(49) Furst, A. L.; Hoepker, A. C.; Francis, M. B. *ACS Cent. Sci.* **2017**, *3*, 110.
(50) Heffernan, A. L.; Thompson, K.; Eaglesham, G.; Vijayasarathy, S.; Mueller, J. F.; Sly, P. D.; Gomez, M. J. *Talanta* **2016**, *151*, 224.
(51) Cunha, S. C.; Pena, A.; Fernandes, J. O. *J. Chromatogr. A* **2015**, *1414*, 10.
(52) Deiminiat, B.; Rounaghi, G. H.; Arbab-Zavar, M. H.; Razavipanah, I. *Sens. Actuators, B* **2017**, *242*, 158.
(53) Soleymani, L.; Fang, Z.; Sargent, E. H.; Kelley, S. O. *Nat. Nanotechnol.* **2009**, *4*, 844.

DOI: 10.1021/jacs.7b06385
J. Am. Chem. Soc. XXXX, XXX, XXX−XXX